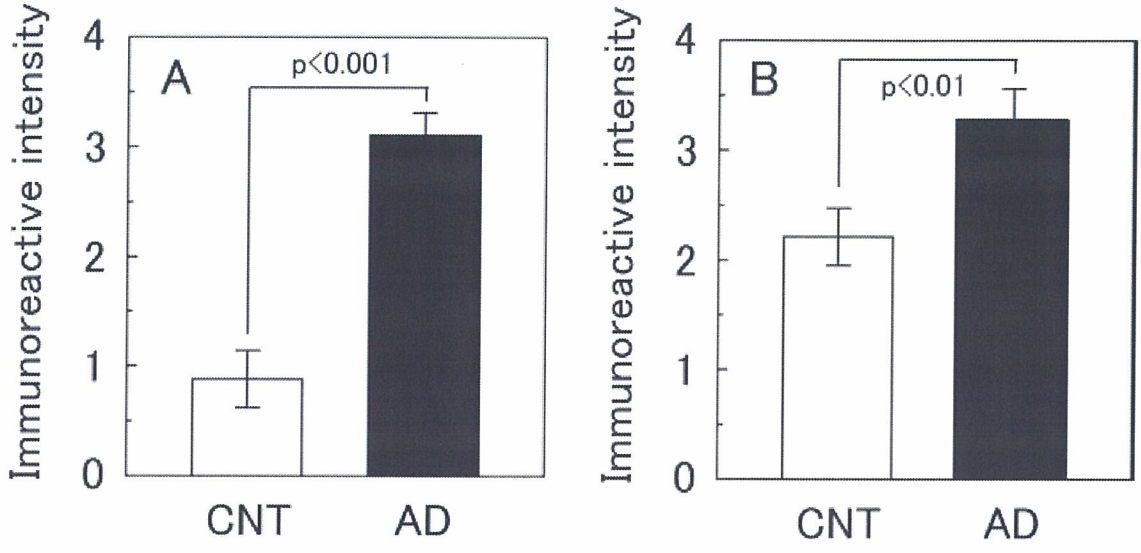

Fig. 4. Immunoreactive intensity of citrullinated proteins and PAD2 in the hippocampi of AD and control brains. The immunoreactivity of citrullinated proteins (**A**) and PAD2 (**B**) in the hippocampus was graded (grade 0 to 4) as described in Materials and Methods. Values are expressed as means ± SEM of 10 AD and nine control subjects. Data were compared by Student's *t*-test.

able all through the hippocampus, both in the AD and in normal brain, but not in the granular layer of the dentate gyrus (Fig. 3C,D). A scoring system adopted to evaluate the degree of PAD2 immunoreactivity in the hippocampus revealed significantly greater immunoreactivity in the AD hippocampus than in its normal counterpart (Fig. 4B). The PAD2-enriched region coincided well with the citrullinated protein-positive regions (Fig. 3A,C). At higher microscopic magnification in the polymorphic layer of dentate gyrus, figures of citrullinated protein-positive cells and PAD2-positive cells were apparent as astrocyte-like cells (Fig. 3E,F). To confirm whether these citrullinated protein- and PAD2-positive cells were astrocytes, we performed double-immunofluorescence staining for citrullinated protein or PAD2 and GFAP, which is an astrocyte-specific marker protein, followed by confocal microscopy (Fig. 5). GFAP-positive fluorescence signals clearly coincided with citrullinated protein-positive signals (Fig. 5A–C) as well as PAD2-positive signals (Fig. 5D–F). Almost all GFAP-positive cells showed immunoreactivity for PAD2, despite a few exceptions. Thus, PAD2 was distributed mainly in astrocytes.

DISCUSSION

We report here, for the first time, the abnormal accumulation of citrullinated proteins and abnormal activation of PAD2 in brain extracts from patients with AD. Citrullinated proteins were barely detectable in normal human brain extracts, although PAD2 was almost universally present.

Previously, we found similar results in the normal rat brain (Asaga and Ishigami, 2000, 2001). Additionally, physiologic insults such as hypoxia and kainic acid administration also resulted in the appearance of citrullinated proteins (Asaga and Ishigami, 2000, 2001; Asaga et al., 2002). PAD2 was present in the rat cerebrum and especially enriched in the dentate gyrus and stratum radiatum of hippocampus, the amygdala, the hypothalamus, and the cortex, but few or no citrullinated proteins were detected in those regions. Under hypoxic conditions (Asaga and Ishigami, 2000) and during kainic acid-evoked neurodegeneration (Asaga and Ishigami, 2001; Asaga et al., 2002), PAD2 became activated in regions undergoing neurodegeneration and functioned to citrullinate various cerebral proteins, indicating the involvement of protein citrullination in neurodegenerative processes. We are convinced that these past and present results confirm the involvement of protein citrullination in human neurodegenerative disease.

In the present study, Western blot analysis revealed numerous citrullinated proteins in the AD hippocampus. We identified citrullinated vimentin and GFAP, which were shown as several independent spots by 2-DE and proteomic analysis (Fig. 2C, Table II). Because protein citrullination results in a decrease in the net positive charge of proteins, each spot must be shown as several pI values with different degrees of citrullination resulting in neutralization of proteins. In the epidermis of mice, we previously identified citrullinated cytokeratins and filaggrin as several independent spots separable by 2-DE and detected by Western blotting (Senshu et al., 1995, 1999). Citrullination of cytokeratins and filaggrin occurs during the latest stages of epidermal differentiation and is thought to play a key role in the cornification process (Senshu et al., 1995). Although citrullination of vimentin and GFAP seems to be much more specific than that of other intracellular proteins, it is still unclear whether citrullination of vimentin and GFAP has physiologically

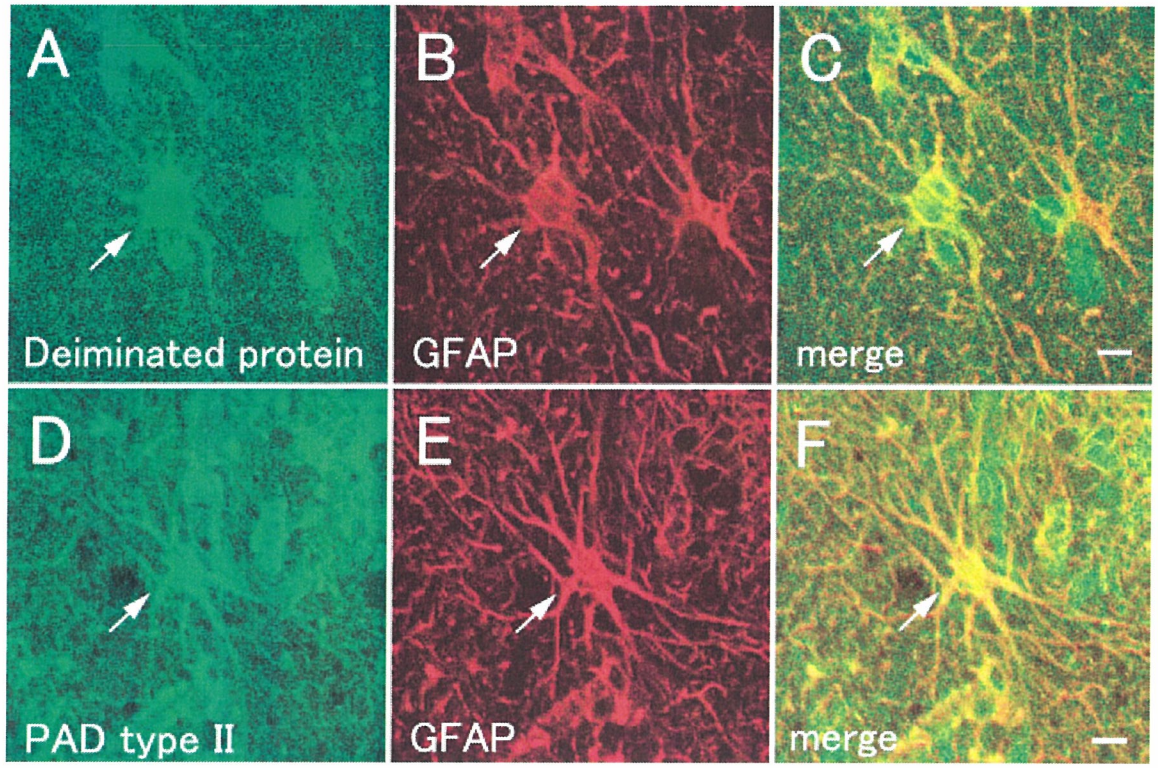

Fig. 5. Identification of citrullinated protein-positive and PAD2-positive cells by double immunofluorescence staining. Sections of AD hippocampus were doubly immunostained with monoclonal anti-GFAP antibody and with polyclonal antimodified citrulline IgG or polyclonal anti-human PAD2 antibody. The primary antibodies were visualized with anti-rabbit Alexa Fluor 488 (green) and anti-mouse Alexa Fluor 594 (red). **A,D:** Alexa 488 (green) for citrullinated protein (A) or PAD2 (D). **B,E:** Alexa 568 (red) for GFAP. **C,F:** Merged views for A/B and D/E, respectively. Arrows indicate coincident position. Scale bars = 5 μm.

important functions in the brains of AD patients. Inagaki et al. (1989) reported that vimentin and GFAP were highly susceptible to the attack of PAD2 in vitro; for example, citrullination of vimentin induced disassembly of intermediate filaments.

Here, we also identified citrullinated MBP, which is an authentic marker of oligodendrocyte, in the AD-afflicted hippocampus. Recently, we found PAD2 localized in a stage-specific, immature oligodendrocyte from a rat's cerebral hemisphere in vitro (Akiyama et al., 1999). Gould et al. (2000) reported that PAD2 cDNA was highly expressed in myelin sheath assembly sites with a combination of subcellular fractionation and suppression subtractive hybridization. Moreover, Moscarello et al. (1994, 2002) reported that PAD enzyme and citrullinated MBP are relatively enriched in immature myelin and that MBP citrullination has an important role in myelin development and in the human demyelinating disease multiple sclerosis. Recently, many investigators have suggested that myelin breakdown may be a contributing factor in the pathology of AD (Bartzokis, 2004; Tian et al., 2004). MBP citrullination might also contribute to the myelin breakdown.

The mechanism(s) by which citrullinated proteins occur in the hippocampus during AD remains unclear. Possibly PAD2 becomes activated, abundant, and functional only in the presence of AD, insofar as the amount of PAD2 increased notably in hippocampi of the AD patients we assessed compared with that in normal subjects. Although PAD2 was also present in hippocampal extracts from normal subjects, that enzyme remained in a steady state during which no enzyme activation occurred. For enzyme activation, the intracellular calcium concentration must become elevated. No other factors can regulate PAD activity in vivo or in vitro, to the best of our knowledge. A loss of neuronal calcium homeostasis leading to increases in the intracellular calcium concentration has been proposed to play a major role in hypoxic and ischemic brain injury (Choi, 1988; Hossmann, 1999). Haun et al. (1992) suggested that an influx of extracellular calcium contributes to astroglial injury during ischemia on the basis of their experimental results with simulated ischemia in a primary culture of astrocytes. Our previous report showed that PAD2 activated and citrullinated various cerebral proteins under hypoxic conditions (Asaga and Ishigami, 2000) and during kainic acid-evoked neurodegeneration (Asaga and Ishigami, 2001; Asaga et al., 2002). Abnormal PAD activation resulted in random protein citrullination, which could then trigger the onset of neurodegenerative disease.

In conclusion, the present data indicate that patients with AD bear an abnormal accumulation of citrullinated

proteins and abnormal activation of PAD2 in the hippocampus. Therefore, citrullinated proteins may be a useful marker for neurodegenerative disease. Moreover, the development of an inhibitory drug specific for PAD2 could conceivably prevent the onset and progression of neurodegeneration.

ACKNOWLEDGMENTS

The excellent editorial assistance of Ms. P. Minick is gratefully acknowledged. This study was supported by a Grant-in-Aid for Scientific Research from the Ministry of Education, Science, and Culture, Japan (to A.I.) and a grant from Health Science Research Grants for Comprehensive Research on Aging and Health supported by the Ministry of Health Labor and Welfare, Japan (to A.I.). Additional support was provided by the SHISEIDO Grant for Scientific Research (to A.I.), the Cosmetology Research Foundation (to A.I.), and the Nakatomi Foundation (to A.I.).

REFERENCES

Akiyama K, Sakurai Y, Asou H, Senshu T. 1999. Localization of peptidylarginine deiminase type II in a stage-specific immature oligodendrocyte from rat cerebral hemisphere. Neurosci Lett 274:53–55.

Asaga H, Ishigami A. 2000. Protein deimination in the rat brain: generation of citrulline-containing proteins in cerebrum perfused with oxygen-deprived media. Biomed Res 21:197–205.

Asaga H, Ishigami A. 2001. Protein deimination in the rat brain after kainate administration: citrulline-containing proteins as a novel marker of neurodegeneration. Neurosci Lett 299:5–8.

Asaga H, Senshu T. 1993. Combined biochemical and immunocytochemical analyses of postmortem protein deimination in the rat spinal cord. Cell Biol Int 17:525–532.

Asaga H, Akiyama K, Ohsawa T, Ishigami A. 2002. Increased and type II-specific expression of peptidylarginine deiminase in activated microglia but not hyperplastic astrocytes following kainic acid-evoked neurodegeneration in the rat brain. Neurosci Lett 326:129–132.

Bartzokis G. 2004. Age-related myelin breakdown: a developmental model of cognitive decline and Alzheimer's disease. Neurobiol Aging 25: 5–18.

Chavanas S, Mechin MC, Takahara H, Kawada A, Nachat R, Serre G, Simon M. 2004. Comparative analysis of the mouse and human peptidylarginine deiminase gene clusters reveals highly conserved non-coding segments and a new human gene, PADI6. Gene 330:19–27.

Choi DW. 1988. Calcium-mediated neurotoxicity: relationship to specific channel types and role in ischemic damage. Trends Neurosci 11:465–469.

Gould RM, Freund CM, Palmer F, Feinstein DL. 2000. Messenger RNAs located in myelin sheath assembly sites. J Neurochem 75:1834–1844.

Haun SE, Murphy EJ, Bates CM, Horrocks LA. 1992. Extracellular calcium is a mediator of astroglial injury during combined glucose-oxygen deprivation. Brain Res 593:45–50.

Hossmann KA. 1999. The hypoxic brain. Insights from ischemia research. Adv Exp Med Biol 474:155–169.

Imparl JM, Senshu T, Graves DJ. 1995. Studies of calcineurin-calmodulin interaction: probing the role of arginine residues using peptidylarginine deiminase. Arch Biochem Biophys 318:370–377.

Inagaki M, Takahara H, Nishi Y, Sugawara K, Sato C. 1989. Ca^{2+}-dependent deimination-induced disassembly of intermediate filaments involves specific modification of the amino-terminal head domain. J Biol Chem 264:18119–18127.

Ishigami A, Ohsawa T, Watanabe K, Senshu T. 1996. All-trans retinoic acid increases peptidylarginine deiminases in a newborn rat keratinocyte cell line. Biochem Biophys Res Commun 223:299–303.

Ishigami A, Kuramoto M, Yamada M, Watanabe K, Senshu T. 1998. Molecular cloning of two novel types of peptidylarginine deiminase cDNAs from retinoic acid-treated culture of a newborn rat keratinocyte cell line. FEBS Lett 433:113–118.

Ishigami A, Asaga H, Ohsawa T, Akiyama K, Maruyama N. 2001. Peptidylarginine deiminase type I, type II, type III and type IV are expressed in rat epidermis. Biomed Res 22:63–65.

Ishigami A, Asaga H, Ohsawa T, Akiyama K, Maruyama N. 2002a. Protein deimination and peptidylarginine deiminase expression during cornification of rat epidermal keratinocytes. Biomed Res 23:145–151.

Ishigami A, Ohsawa T, Asaga H, Akiyama K, Kuramoto M, Maruyama N. 2002b. Human peptidylarginine deiminase type II: molecular cloning, gene organization, and expression in human skin. Arch Biochem Biophys 407:25–31.

Katzman R. 1986. Alzheimer's disease. N Engl J Med 314:964–973.

Keller JN, Hanni KB, Markesbery WR. 2000. Impaired proteasome function in Alzheimer's disease. J Neurochem 75:436–439.

Kubilus J, Baden HP. 1983. Purification and properties of a brain enzyme which deiminates proteins. Biochim Biophys Acta 745:285–291.

Kubilus J, Waitkus RF, Baden HP. 1980. Partial purification and specificity of an arginine-converting enzyme from bovine epidermis. Biochim Biophys Acta 615:246–251.

Laemmli UK. 1970. Cleavage of structural proteins during the assembly of the head of bacteriophage T4. Nature 227:680–685.

Lamensa JW, Moscarello MA. 1993. Deimination of human myelin basic protein by a peptidylarginine deiminase from bovine brain. J Neurochem 61:987–996.

Lowry OH, Rosebrough NJ, Farr AL, Randall RJ. 1951. Protein measurement with the phenol reagent. J Cell Biol 193:265–275.

Maccioni RB, Munoz JP, Barbeito L. 2001. The molecular bases of Alzheimer's disease and other neurodegenerative disorders. Arch Med Res 32:367–381.

Moscarello MA, Wood DD, Ackerley C, Boulias C. 1994. Myelin in multiple sclerosis is developmentally immature. J Clin Invest 94:146–154.

Moscarello MA, Pritzker L, Mastronardi FG, Wood DD. 2002. Peptidylarginine deiminase: a candidate factor in demyelinating disease. J Neurochem 81:335–343.

Nakashima K, Hagiwara T, Ishigami A, Nagata S, Asaga H, Kuramoto M, Senshu T, Yamada M. 1999. Molecular characterization of peptidylarginine deiminase in HL-60 cells induced by retinoic acid and 1α, 25-dihydroxyvitamin D_3. J Biol Chem 274:27786–27792.

National Institute on Aging, and Reagan Institute Working Group on Diagnostic Criteria for the Neuropathological Assessment of Alzheimer's Disease. 1997. Consensus recommendations for the postmortem diagnosis of Alzheimer's disease. Neurobiol Aging 18:S1–S2.

Nishijyo T, Kawada A, Kanno T, Shiraiwa M, Takahara H. 1997. Isolation and molecular cloning of epidermal- and hair follicle-specific peptidylarginine deiminase (type III) from rat. J Biochem (Tokyo) 121:868–875.

Ohsawa T, Ishigami A, Akiyama K, Asaga H. 2001. Immunocytochemical localization of peptidylarginine deiminase type III, trichohyalin and deiminated trichohyalin in infant rat dorsal skin hair follicle. Biomed Res 22:91–97.

Rogers GE, Simmonds DH. 1958. Content of citrulline and other amino acids in a protein of hair follicles. Nature 182:186–187.

Rus'd AA, Ikejiri Y, Ono H, Yonekawa T, Shiraiwa M, Kawada A, Takahara H. 1999. Molecular cloning of cDNAs of mouse peptidylarginine deiminase type I, type III and type IV, and the expression pattern of type I in mouse. Eur J Biochem 259:660–669.

Senshu T, Sato T, Inoue T, Akiyama K, Asaga H. 1992. Detection of citrulline residues in deiminated proteins on polyvinylidene difluoride membrane. Anal Biochem 203:94–100.

Senshu T, Akiyama K, Kan S, Asaga H, Ishigami A, Manabe M. 1995. Detection of deiminated proteins in rat skin: probing with a monospecific antibody after modification of citrulline residues. J Invest Dermatol 105:163–169.

Senshu T, Akiyama K, Ishigami A, Nomura K. 1999. Studies on specificity of peptidylarginine deiminase reactions using an immunochemical probe that recognizes an enzymatically deiminated partial sequence of mouse keratin K1. J Dermatol Sci 21:113–126.

Smith MA. 1998. Alzheimer disease. Int Rev Neurobiol 42:1–54.

Tarcsa E, Marekov LN, Mei G, Melino G, Lee S-C, Steinert PM. 1996. Protein unfolding by peptidylarginine deiminase. Substrate specificity and structural relationships of the natural substrates trichohyalin and filaggrin. J Biol Chem 271:30709–30716.

Terakawa H, Takahara H, Sugawara K. 1991. Three types of mouse peptidylarginine deiminase: characterization and tissue distribution. J Biochem (Tokyo) 110:661–666.

Tian J, Shi J, Bailey K, Mann DM. 2004. Relationships between arteriosclerosis, cerebral amyloid angiopathy and myelin loss from cerebral cortical white matter in Alzheimer's disease. Neuropathol Appl Neurobiol 30:46–56.

Toda T, Kaji K, Kimura N. 1998. TMIG-2DPAGE: a new concept of two-dimensional gel protein database for research on aging. Electrophoresis 19:344–348.

Towbin H, Staehelin T, Gordon J. 1979. Electrophoretic transfer of proteins from polyacrylamide gels to nitrocellulose sheets: procedure and some applications. Proc Natl Acad Sci U S A 76:4350–4354.

Tsuchida M, Takahara H, Minami N, Arai T, Kobayashi Y, Tsujimoto H, Fukazawa C, Sugawara K. 1993. cDNA nucleotide sequence and primary structure of mouse uterine peptidylarginine deiminase. Detection of a 3′-untranslated nucleotide sequence common to the mRNA of transiently expressed genes and rapid turnover of this enzyme's mRNA in the estrous cycle. Eur J Biochem 215:677–685.

Vincent SR, Leung E, Watanabe K. 1992. Immunohistochemical localization of peptidylarginine deiminase in the rat brain. J Chem Neuroanat 5:159–168.

Watanabe K, Senshu T. 1989. Isolation and characterization of cDNA clones encoding rat skeletal muscle peptidylarginine deiminase. J Biol Chem 264:15255–15260.

Watanabe K, Akiyama K, Hikichi K, Ohtsuka R, Okuyama A, Senshu T. 1988. Combined biochemical and immunochemical comparison of peptidylarginine deiminases present in various tissues. Biochim Biophys Acta 966:375–383.

Kidney International, Vol. 68 (2005), pp. 84–95

Citrullination preferentially proceeds in glomerular Bowman's capsule and increases in obstructive nephropathy

DONGYUN FENG, TOSHIYUKI IMASAWA, TADASUKE NAGANO, MASARU KIKKAWA, KAORI TAKAYANAGI, TAKAKO OHSAWA, KYOICHI AKIYAMA, AKIHITO ISHIGAMI, TOSIFUSA TODA, TETSUYA MITARAI, TAKEO MACHIDA, and NAOKI MARUYAMA

Department of Molecular Pathology, Tokyo Metropolitan Institute of Gerontology, Tokyo, Japan; Department of Bioactivity Regulation, Tokyo Metropolitan Institute of Gerontology, Tokyo, Japan; Department of Proteome Analysis, Tokyo Metropolitan Institute of Gerontology, Tokyo, Japan; Department of Internal Medicine and Division of Immunopathology, Clinical Research Center, Chiba-East National Hospital, Chiba, Japan; Division of Nephrology, Saitama Medical Center, Saitama Medical School, Saitama, Japan; and Department of Regulation Biology, Faculty of Science, Saitama University, Saitama, Japan

Citrullination preferentially proceeds in glomerular Bowman's capsule and increases in obstructive nephropathy.

Background. Peptidylarginine deiminases (PADs) are a group of posttranslational modification enzymes that citrullinate (deiminate) protein arginine residues, yielding citrulline residues. Citrullination of arginine residues abolishes their positive charge, markedly altering their structure. We undertook this study to investigate the actions of PADs in the kidney.

Methods. In male rats, we ligated the unilateral ureter, then analyzed the obstructed and contralateral kidneys 1 week later. Controls were rats simultaneously given sham operations. In another experiment, we ligated unilateral ureters of eight rats, four of which received a ureter-bladder anastomosis 1 week later. These rats were subjected to histologic examinations 5 weeks after unilateral ureteral obstruction (UUO).

Results. Reverse transcription-polymerase chain reaction (RT-PCR) revealed that, of PADs (type I, II, III, and IV), only PAD type II was expressed in kidneys. Western blot study showed that PAD type II expression and citrullinated protein content increased greatly in kidneys that underwent unilateral ureteral ligation compared to that in contralateral or sham-operated kidneys. Immunohistochemical analyses revealed that PAD type II was preferentially expressed by parietal epithelial cells and that only in Bowman's capsule were proteins citrullinated. Additionally, these PAD type II and citrullinated proteins in obstructed nephropathy were significantly attenuated by the release of the obstruction. Proteome analysis revealed that one of citrullinated proteins in the kidney should be actin.

Conclusion. This result indicates that PAD type II and citrullinated proteins are suitable markers of Bowman's capsule. Not only are these markers preferentially expressed in Bowman's capsules but their expression is also increased in damaged kidneys by UUO, features that promise the further clarification of kidney diseases.

Key words: obstructive nephropathy, Bowman's capsule, parietal epithelial cells, citrullination, peptidylarginine deiminases (PAD), posttranslational modification.

Received for publication August 26, 2004
and in revised form December 7, 2004, and January 15, 2005
Accepted for publication January 28, 2005

Bowman's capsule, the outer epithelial wall of the glomerular corpuscle, surrounds glomeruli's loops and lobules. In normal conditions, parietal epithelial cells constituting Bowman's capsule are simple, flat squamous structures. However, the conformation of parietal epithelial cells variously changes in response to such pathologic stimuli as ischemia, hypertension, and inflammation. The result is thickening of the parietal epithelium, and as these parietal epithelial cells proliferate, they become cuboidal and form the glomerular crescents that typify some types of glomerulonephritis. Although Bowman's capsule frequently develops this conformation in patients with kidney diseases, few studies have dealt with it. To date, protein gene product 9.5 is the only known specific marker for Bowman's capsule but this also localizes nerve fibers around arteries [1].

Peptidylarginine deiminase (PADs) are posttranslational modification enzymes that convert protein arginine to citrulline residues [2, 3]. Enzymatic citrullination (deimination) abolishes the positive charge of protein molecules inevitably causing significant alterations in their structure and function [4, 5]. These PADs are distinct from nitric oxide synthetase (NOS) and arginine deiminase, which convert free arginine to citrulline. Mammals have four types of PADs, designated as type I, type II, type III, and type IV [6]. Functionally, PADs have been linked with the pathogenesis of some diseases; for example, PAD type IV is the proposed cause of rheumatoid arthritis and multiple sclerosis [4, 7–9].

Multiple mammalian tissues contain PADs [10] and PAD expression has tissue specificity; for examples, although all PADs are present in epidermis [6], only PAD type II is exclusively expressed in brain [9]. Moreover, citrullination by all PADs shows a definite requirement for Ca^{2+} [11]. Although the mRNA of PAD type II and type IV was previously identified in the rat kidney [6], whether citrullinated proteins also occupy the kidneys

remains uncertain. Therefore, in this study, we used a rat model of kidneys damaged by unilateral ureteral obstruction (UUO) to assess the expression of PADs and the presence of citrullinated proteins. As a result, we present here the first report that specific markers are preferentially expressed in glomerular Bowman's capsules of the kidney and that their expression increases in response to kidney damage.

METHODS

Animals

Male Sprague-Dawley rats (Charles River Breeding Laboratories, Wilmington, MA, USA), weighing 150 to 180 g, were used in this study. Animals were fed standard rodent chow and were given water ad libitum. After intraperitoneal administration of pentobarbital (5.0 mg/kg body weight) (Dainippon Pharmaceutical Co., Ltd, Osaka, Japan), anesthetized animals underwent either left proximal ureteral ligation ($N = 6$) or, simultaneously, a sham operation ($N = 6$). One week later, the obstructed (left UUO) kidneys and the contralateral unobstructed (right) kidneys as well as normal kidneys from sham-operated animals were harvested from these rats. Before removal, the kidneys were well perfused with approximately 100 mL of normal saline to remove circulating blood cell fractions or adherent cells. Blood samples were centrifuged (6000 rpm for 3 minutes) to separate serum for biochemical measurements. Blood urea nitrogen (BUN) and serum creatinine were measured by urease-ultraviolet and enzymatic reaction, respectively (SRL, Inc., Tokyo Japan).

Ureter-bladder anastomosis

In another animal experiment, eight male Sprague-Dawley rats (150 to 180 g) were subjected to left UUO. Four rats of them underwent operation to make ureter-bladder anastomosis 1 week after the ureteral ligation. For building the anastomosis, a sterile and nontoxic polyethylene tube (external diameter 1 mm) (PE-90) (Clay Adams Intradermic Inc., Sparks, MD, USA) was inserted to dilated left ureter and the bladder and fixed securely by silk ligation. These rats were histologically analyzed 5 weeks after the first UUO operation. Simultaneously, the other four rats with UUO for 5 weeks were examined.

Reverse transcriptase-polymerase chain reaction (RT-PCR)

The kidney cortex was dissected and homogenized in Isogen (Nippon Gene, Tokyo, Japan) to isolate total RNA, followed by treatment with RNase-free DNase I (Nippon Gene) to remove DNA contamination according to the supplier's protocol. The amount of RNA extracted was estimated by spectrophotometer. RT-PCR was performed with a Takara mRNA Selective PCR Kit (Takara Shuzo Co., Ltd., Kyoto, Japan) according to the manufacturer's instructions. RT was performed using antisense oligonucleotide primers. The primers of rat PADs type I, type II, type II, type IV, and glyceraldehyde-3-phosphate dehydrogenase (GAPDH) were designed as described previously [6]. The sense and antisense primers were for rat PAD type I, 5′-AGGTATTAGAA GATGGTGGGGTAGG-3′ and 5′-CCCAACCTTCTC ATCCCCCTTTA-3′ (expected size 631 bp) [12]; for rat PAD type II, 5′-ATTCAAGATAGACCAGGAGGA CCAG-3′ and 5′-CAGAATAGGAAGGCCAGTGTCA GAA-3′ (expected size 428 bp) [10]; for rat PAD type III, 5′- CCTTGGCTTGTGCTTCCTATGGT-3′ and 5′-TCCCTCCCTTCTCCCAGTATGTG-3′ (expected size 648 bp) [6]; for rat PAD type IV, 5′-CGCTC CTGGCAGCCTCCCTCGAGGA-3′ and 5′-CAGCAT CTCTAAGCAGGACTGAGTT-3′ (expected size 205 bp) [12]; and for rat GAPDH, 5′-GTGAAGGTCGGT GTGAACGGAT-3′ and 5′-GCCGCCTGCTTCACCAC CTTCTT-3′ (expected size 788 bp) [6]. We also followed PCR conditions as reported with some modifications [6]; 30 minutes at 50°C, and then 15 minutes at 95°C, followed by 31 or 32 cycles at 94°C for 30 seconds, 60°C for 30 seconds, and 72°C for 1 minute, and a terminal extension (72°C, 10 minutes). We used the same templates from each experimented kidney for RT-PCR. The condition of templates was checked by amplification for GAPDH. A positive control for RT-PCR of PADs was obtained from rat epidermis where all PADs are expressed [6]. For RT-PCR of PAD type II, mRNA was amplified by mixing primers of PAD type II and GAPDH. PCR products were visualized by agarose gel electrophoresis with ethidium bromide staining. Bands were quantified by densitometry. GAPDH mRNA was analyzed as an internal control, and relative amounts of PAD type II expression were calculated.

Extraction of proteins and Western blotting

Specimens from the renal cortex containing ~500 mg of protein were sonicated in extraction buffer [20 mmol/L Tris-HCl, 150 mmol/L NaCl, 2 mmol/L ethylenediaminetetraacetic acid (EDTA), 1% Nonidet P40, 50 mmol/L NaF, and 1 mmol/L Na_3VO_4] with protease inhibitor cocktail (Roche, Mannheim, Germany) to extract proteins. Insoluble materials were removed by centrifugation at 15,000 rpm for 10 minutes. The supernatants of samples were incubated with the sample buffer [125 mmol/L Tris-HCl, pH 6.8, 20% glycerol, 10% 2-mercaptoethanol, 4% sodium dodecyl sulfate (SDS), 0.005% bromophenol blue (BPB), and 0.005% methylene blue] and heated in boiling water for 5 minutes. Protein concentrations were estimated with

the BCA Protein Assay Reagent Kit (Pierce, Rockford, IL, USA). Aliquots (30 μg of crude kidney homogenate) were resolved by SDS-polyacrylamide gel electrophoresis (PAGE) (10% gel) and transferred to polyvinylidene difluoride (PVDF) membranes (Millipore, Bedford, MA, USA). The membranes were blocked with 5% nonfat dried milk in Tris-bufferd saline (100 mmol/L Tris-HCl/1.4 mol/L NaCl, pH 7.5)/0.1% Tween-20 (TBST) for 1 hour at room temperature before reaction with the first antibodies. For detection of PAD type II, the blot was incubated with rabbit antirat PAD type II antiserum (×2000) [13]. As a control, the other membrane was incubated with the same concentration of rabbit serum instead of anti PAD type II antibody. For detection of deiminated proteins, we followed a previously reported protocol [14]. Briefly, citrulline residues on the blot were chemically modified by overnight incubation at 37°C in 0.0125% $FeCl_3$, 2.3 mol/L H_2SO_4, 1.5 mol/L H_3PO_4, 0.25% diacetyl monoxime, 0.125% antipyrine, and 0.25 mol/L acetic acid (modification medium). As a control, the other membrane was incubated in the medium free from diacetyl monoxime and antipyrine. The blot was then incubated with a monospecific IgG to modified citrulline (0.125 g/mL) [14]. After reaction with the first antibody, the bound antibodies were detected using horseradish peroxidase–conjugated goat anti-rabbit IgG (PAD type II ×5000, citrulline ×10000) (Bio-Rad Laboratories, Hercules, CA, USA) and enhanced cheminluminescence (ECL) Western blotting detection reagents (Amersham Biosciences Corp., Piscataway, NJ, USA) according to the manufacturer's instructions. To visualize total proteins, Coomassie brilliant blue (CBB) staining was then performed with a Quick-CBB kit (Wako Pure Chemical Industries, Ltd., Osaka, Japan). The bands of PAD type II proteins were quantified by densitometry. The intensity of each band was standardized by the mean of sham-operated group.

Light microscopy

One week after the operation, we performed histologic analyses of the kidneys, which had been sufficiently perfused for removal of circulating cells from the glomeruli. For light microscopy, tissue samples were then fixed with 3% formalin-phosphate-buffered saline (PBS) and embedded in paraffin. After sectioning, the tissues were stained with periodic acid-methenamine-silver (PAM).

PAD staining

Tissue samples from the rats were embedded in 22-oxacalcitriol (OCT) compound (Miles Scientific, Naperville, IL, USA), and quickly frozen in dry ice-acetone. Cryostat sections (4 μm) were fixed in cold acetone for 10 minutes. PAD type II was visible after staining for the indirect fluorescent method. After being washed with PBS, the sections were incubated with rabbit anti-PAD type II antiserum [13], followed by rinsing in PBS and incubation at 37°C for 60 minutes with rhodamine-conjugated sheep antirabbit IgG antibody (ICN Pharmaceuticals, Inc., Aurora, OH, USA). As controls, the tissues were incubated with rabbit serum instead of the first antibody. The sections were rinsed again in PBS, mounted with SlowFade antifade kits (Molecular Probes, Eugene, OR, USA). No positive staining occurred in control tissues. The degrees of PAD type II staining were calculated by two methods. At first, we counted the number of positive glomeruli and expressed them as the percentage of all visible glomeruli. In addition, the area positive for PAD type II in the whole Bowman's capsule of a glomerulus was scored semiquantitatively from 0 to 4: 0, negative staining; 1, less than 25%; 2, 25% to 50%; 3, 50% to 75%; and 4, 75% to 100%. We evaluated more than 30 glomeruli a section and calculated mean value of each section.

Detection of citrullinated protein in situ

Immunostaining of citrullinated proteins was performed by using antimodified citrulline IgG monoclonal antibody and a Vectastain Elite ABC kit (PK-6101) (Vector Laboratories, Inc., Burlingame, CA, USA) as described previously [15]. This antibody reacts with citrulline residues that are chemically modified. Briefly, cryosections were post-fixed with 2.5% glutaraldehyde in PBS and then incubated in the modification medium (0.0125% $FeCl_3$, 2.3 mol/L H_2SO_4, 1.5 mol/L H_3PO_4, 0.25% diacetyl monoxime, 0.125% antipyrine, and 0.25 mol/L acetic acid) at 37°C overnight to modify citrulline residues in situ. Control sections were incubated in the medium free from diacetyl monoxime and antipyrine. After washing with PBS, the sections were incubated with 2% bovine serum albumin (BSA)-PBS at room temperature for 30 minutes to block nonspecific reactions. Then, they were reacted with anti-modified citrulline antibody at 37°C for 2 hours. After washing with PBS, the sections were next incubated with biotinylated antirabbit antibody (Vector Laboratories, Inc) at room temperature for 30 minutes. The sensitivity of this immunostaining was amplified by Elite ABC mixture. Finally, we incubated sections in a peroxidase substrate solution made from buffered substrate for liquid diaminobenzidine (DAB) (Dako Corporation, Carpinteria, CA, USA) and liquid DAB chromogen (Dako Corporation) until the desired stain intensity developed. Staining intensity of citrullinated proteins were analyzed by same ways as scoring of PAD type II staining.

Preparation of protein and two-dimensional gel electrophoresis

Proteins in the kidney were extracted with extraction buffer (8.5 mol/L urea, 0.2% SDS, 2% Triton X-100, 3% 2-mercaptoethanol, 0.8% pharmalyte 3-10, 1 mmol/L Na_3VO_4, and protease inhibitor cocktail), homogenized and centrifuged for 10 minutes at 15,000 rpm. The cytosolic fraction (supernatant) was separated by two dimensional electrophoresis performed in an immobilized pH gradients (IPG)-isoelectric focusing (IEF)/SDS-PAGE system according to the standard protocol found on the Web page *http://proteome.tmig.or.jp/2D/2DE_method.html* with minor modification. In brief, IEF was performed on IPG, pH 4 to 7, 180 mm (Amersham Biosciences AB, Uppsala, Sweden)] with CoolPhorestar model 3610 Horizontal IEF apparatus (Anatech, Tokyo, Japan). The IPG gels were incubated in rehydrating buffer [6 mol/L urea, 2 mol/L thiourea, 13 mmol/L dithiothreitol (DTT), 0.8% pharmalyte 3-10, 2.5 mmol/L acetic acid, 0.0025% (wt/vol) orangeG, and 2% (vol/vol) Triton X-100] overnight. The protein samples (100 μg) were absorbed in a small piece of filter paper and they were applied near the cathode wick on the IPG gel. After 600 to 700 V/hour at 20°C of electrofocusing, the IPG gels were incubated for 30 minutes in equilibration buffer [6 mol/L urea, 33 mmol/L DTT, 25 mmol/L Tris-HCl (pH6.8), 2% (wt/vol) SDS, 0.0025% (wt/vol) BPB, and 30% (vol/vol) glycerol], followed by a 20-minute incubation in equilibration buffer [25 mmol/L Tris-HCl, pH 6.8, 2% (wt/vol) SDS, 0.0025% (wt/vol) BPB, 30% (vol/vol) glycerol, and 0.243 mol/L idoacetamide].

Separation of the second dimension was performed in precast 7.5% SDS/polyacrylamide gel [Tris/Tricine, 200 × 200mm (Anatech)] using the CoolPhoreStar SDS-PAGE Dual-200 vertical slab gel electrophoresis apparatus (Anatech). SDS-PAGE was carried out at 25 mA per gel for 5 hours. After electrophoresis, proteins were stained with Sypro ruby gel stain (Molecular Probes, Inc.) following the manufacturer's protocol and visualized by Molecular Imager FX (Bio-Rad, Tokyo, Japan).

Mass spectrometry

Protein spots exicised from two-dimensional electrophoresed gels were destained and subjected to digestion with sequence-grade modified trypsin (Sigma Chemical Co., St. Louis, MO, USA) at 30°C overnight. The digested peptides was mixed with equal volumes of matrix (10 mg/mL a-cyano-4-hydroxy-trans-cinnamic acid in 50% acetonitrile, 40% methanol, and 0.1% trifluoroacetic acid) and applied to a matrix-assisted laser desorption/ionization (MALDI) targed plate. Pepetide mass was analyzed using AXIMA CFR MALDI time-of-flight (MALDI-TOF) mass spectrometer (Shimadzu, Kyoto, Japan). The spectra were obtained in the positive-ion reflector mode with delayed extraction. External calibration was performed using des-Arg-bradykinin $[M + H]^+ = 904.5$ (monoisotopic), and adrenocorticotropic hormone (ACTH) $[M + H]^+ = 2465.7$ (monoisotopic). Peptide mass fingerprinting [phenylmethylsulfonyl fluoride (PMSF)] database search was performed by sending the list of observed masses to MASCOT search engine *http://www.matrixscience.com/*

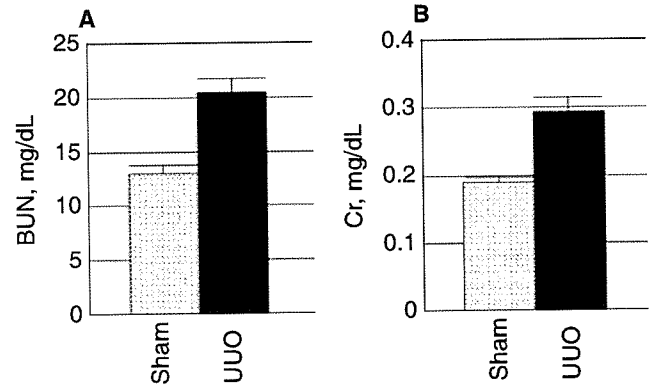

Fig. 1. Biochemical parameters 1 week after operations. Blood urea nitrogen (BUN) levels (*A*) were significantly increased in the unilateral ureteral obstruction (UUO)-treated rats (■) (20.5 ± 1.25 mg/dL) above those in recipients of sham-operation (□) (12.9 ± 0.83 mg/dL) ($P < 0.01$). Similarly, serum creatinine (Cr) (*B*) of UUO group (■) (0.29 ± 0.02 mg/dL) was significantly elevated compared with that of the sham-operated group (□) (0.19 ± 0.01 mg/dL) ($P < 0.01$).

Statistical analysis

All values are expressed as means ± SEM. Statistical significance between groups was determined by the unpaired *t* test. *P* values less than 0.05 were considered statistically significant.

RESULTS

Renal damage was induced by UUO

One week after surgery to place ureteral obstructions in the left kidneys of rats ($N = 6$), serum levels of BUN and creatinine were measured to confirm whether the UUO procedure caused subsequent renal failure. Serum BUN levels in these animals were significantly greater than those in sham-operated group ($N = 6$) (20.5 ± 1.25 mg/dL vs. 12.9 ± 0.83 mg/dL) ($P < 0.001$) (Fig. 1). Similarly, serum creatinine levels in the UUO group exceeded those in the sham-operated group (0.29 ± 0.02 mg/dL vs. 0.19 ± 0.01 mg/dL) ($P < 0.01$) (Fig. 1).

Histologically, renal tissues of sham-operated rats appeared normal under the light microscope (Fig. 2A and B). One week after surgery, glomeruli in the right (contralateral), unobstructed kidneys of UUO group were almost normal (Fig. 2C), whereas glomeruli of the obstructed left kidneys were shrunken, with cuboidal

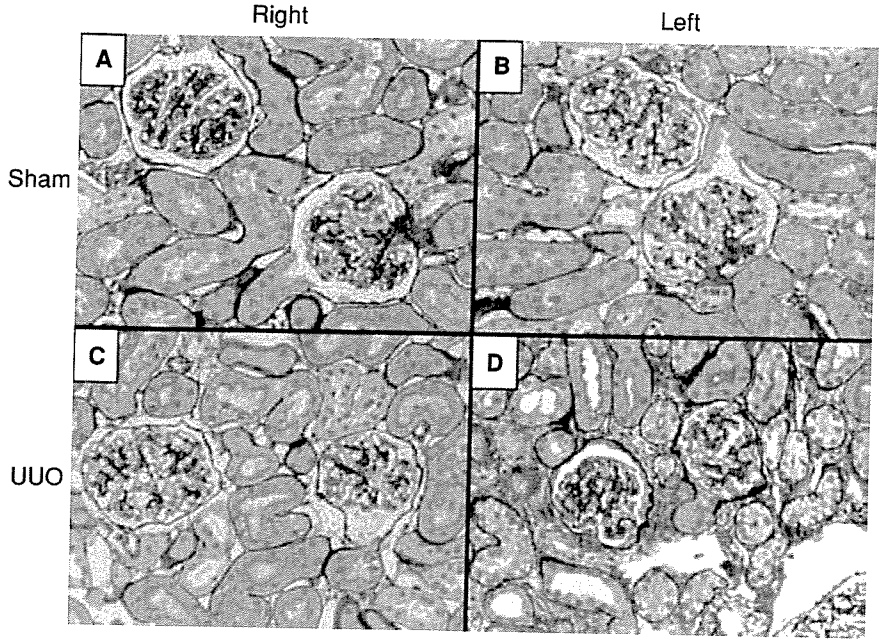

Fig. 2. Light microscopic findings 1 week after the operations. Under the light microscope, periodic acid-methenamine-silver (PAM) staining of kidney sections 1 week after unilateral ureteral obstruction (UUO) or sham-operation (Sham) showed that glomeruli and interstitium from right kidneys (*A*) and left kidneys (*B*) of sham-operated rats were normal. Similarly, unobstructed right kidneys from rats whose left kidneys received UUO had normal glomeruli (*C*). However, in UUO-treated left kidneys (*D*), not only interstitial expansion was observed, but also thickened Bowman's capsules and cuboidal changes of parietal epithelial cells (original magnifications ×200).

parietal epithelium and fibrosis around Bowman's capsule (Fig. 2D). The expansion of interstitial area was also observed in the obstructed kidneys. These results present a clear picture of surgically induced obstructive nephropathy.

PAD type II mRNA was detected in kidney samples

The expression of PAD mRNAs was assessed by RT-PCR using individual primers for rat PAD type I, type II, type III, and type IV. However, no mRNA of PAD type I or type III was detected in samples from obstructed, contralateral or healthy control kidneys (Fig. 3B and C, lanes 1 to 4). Because mRNAs of the same samples from experimentally manipulated kidneys were amplified by primers of GAPDH (Fig. 3A, upper bands of lanes 1 to 5), and positive controls from epidermis expressing all PADs (Fig. 3A to D, lane 5) were also amplified by primers of PAD type I and type III, we verified that these samples were suitable for detection of the mRNA of interest. Like PAD types I and III, PAD type IV mRNA was seldom expressed in obstructed, contralateral or healthy control kidneys (Fig. 3D, lanes 1 to 4). Again, the suitability of extracted mRNA and primers of PAD type IV (Fig. 3A to D, lane 5) for these assays was confirmed. In contrast to the foregoing results in which PAD type I, III, and IV were not expressed, PAD type II mRNA was detected in all samples from the cortexes of normal as well as damaged kidneys (Fig. 3A, lanes 1 to 4). Relative PAD type II mRNA expression (PAD type II/GAPDH) is the highest in the left kidney with the obstruction (Fig. 3E).

Amounts of PAD type II protein increased in obstructed kidneys

Next, expression of PAD type II was examined by Western blot analysis. As shown in Figure 4, PAD type II protein was only minimally detectable in kidneys of sham-operated rats and the right contralateral kidneys of the UUO group (Fig. 4A, sham left and UUO right). However, PAD type II protein of approximately 70 kD was observed in the left kidneys of the UUO group (Fig. 4A, UUO left). The specificity of rabbit anti-PAD type II antibody used to identify the protein was reconfirmed when no bands were detectable with rabbit serum used as a first antibody instead of anti-PAD type II antibody (Fig. 4C). Additionally, the extracted proteins were stained by CBB (Fig. 4B and D). When protein bands were quantified by densitometry, PAD type II protein was significantly increased in obstructed kidneys (Fig. 4E).

Obstructed kidneys developed large increases in citrullinated proteins

The expression of the PAD type II does not always catalyze citrullination, because this reaction requires Ca^{2+}. However, Western blot analysis using specific antibody against modified citrulline residues successfully yielded bands of approximately 70 kD, 60 kD, and 40 kD, denoting the presence of citrullinated proteins on chemically treated membranes only in obstructed kidneys of the UUO group (Fig. 5A, UUO left). To the contrary, in the kidneys of sham-operated rats and contralateral kidneys of the UUO animals, no such bands appeared (Fig. 5A, sham left and UUO right). Because this antibody does not react with unmodified citrulline, we can certify the

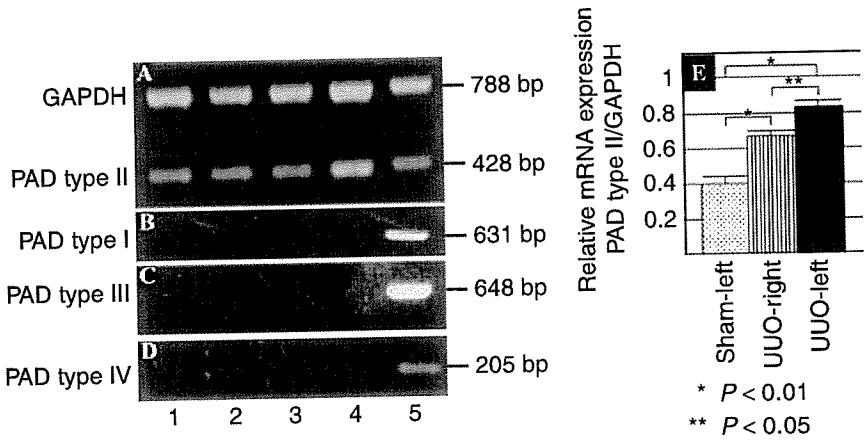

Fig. 3. Expression of glyceraldehyde-3-phosphate dehydrogenase (GAPDH) (*A*), peptidylarginine deiminases (PAD) type I (*B*), type II (A), type III (*C*), and type IV (*D*) transcripts in rat kidneys. Total RNA was isolated from the cortexes of rat kidneys, and the same templates from experimented kidneys were amplified by reverse transcription-polymerase chain reaction (RT-PCR) using each primer. Lane 1, right kidney with sham-operation; lane 2, left kidney with sham-operation; lane 3, right (contralateral) kidney with unilateral ureteral obstruction (UUO) treatment; lane 4, left kidney (obstructed) kidney with UUO; lane 5, positive control from rat epidermis. Expected sizes of amplified sequences based on primer design were 631 bp for PAD type I, 428 bp for PAD type II, 648 bp for PAD type III, 205 bp for PAD type III, and 788 bp for GAPDH. All PADs transcripts were observed in epidermal samples and all samples were amplified by primers of GAPDH. PAD type II mRNA was detected only in kidney tissue, regardless of obstruction or lack thereof (A). PAD type I (B), III (C), and IV (D) mRNA were merely detected in samples from obstructed, contralateral, or healthy control kidneys. Relative amount of PAD type II mRNA expression (PAD type II/GAPDH) is the highest in left kidneys with the obstruction (*E*). Values are mean ± SEM.

specificity of this antibody by staining membranes without chemical treatment. As shown in Fig. 5C, no bands emerged on the membrane without chemical modification. The extracted proteins were stained by CBB staining (Fig. 5B and D).

PAD type II protein was preferentially expressed in parietal epithelial cells of kidneys damaged by obstruction but not in normal kidneys

By immunohistochemical analysis, PAD type II expression was barely noticeable along the parietal epithelia of normal rat kidneys (Fig. 6A and B, Sham) or in unobstructed kidneys (Fig. 6C, UUO right). On the other hand, PAD type II expression was marked in parietal epithelia of tissue undergoing obstructive nephropathy 1 week after the UUO operation (Fig. 6D, UUO left). No PAD type II expression was observed except on glomerular parietal epithelial cells. As shown in Table 1, 1 week after UUO, intensity of PAD type II expression in Bowman's capsules and percentages of PAD type II–positive glomeruli were significantly increased in left kidneys of UUO group (UUO left 1 week) compared with those of contralateral kidneys (UUO right 1 week) or sham-operated kidneys (Sham left).

Citrullinated protein is preferentially present along Bowman's capsule

When we proceeded with staining to identify citrullinated proteins in situ, almost no citrullinated proteins appeared in kidneys of sham-operated rats (Fig.7A and B). Sometimes, a few citrullinated proteins lay along Bowman's capsule in a very small number of glomeruli of the sham-operated group. Similarly, citrullinated proteins were scarce in right contralateral kidneys of the UUO group (Fig. 7C). To the contrary, citrullinated proteins were visible along Bowman's capsule of the obstructed left kidneys (Fig. 7D). When we stained rat kidney tissues without chemical treatment by the modification medium, no positive staining was seen at all (Fig. 7E to H). Therefore, the specificity of the antibody used was reconfirmed histochemically, and this procedure showed that PAD type II and citrullinated proteins both lodged preferentially along Bowman's capsules of damaged kidneys by UUO. One week after UUO, staining intensity for citrullinated proteins in Bowman's capsules and percentages of positive glomeruli were markedly higher in the left obstructed kidneys of UUO group than right unobstructed kidneys or sham-operated kidneys (Table 1).

Citrullination decreased by the release of ureteral obstruction

To investigate whether citrullination reflects kidney damages by UUO, ureter-bladder anastomosis was made 1 week after the UUO operation. Glomeruli of the left kidneys with UUO for 5 weeks had cuboidal parietal epithelium and periglomerular fibrosis around Bowman's capsule (Fig. 8A). Four weeks after the release of ureteral obstruction, glomeruli returned to normal, and its parietal epithelium became flat (Fig. 8B). This light

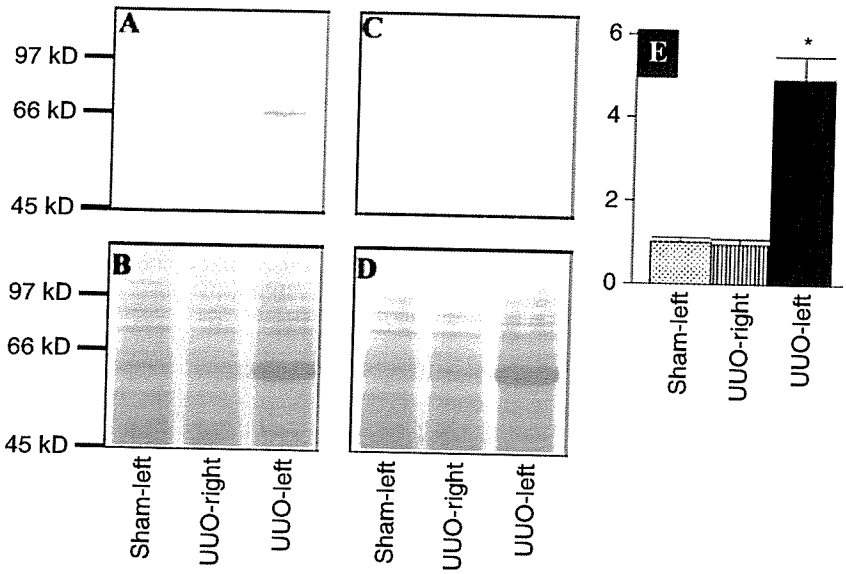

Fig. 4. Western blot for peptidylarginine deiminases (PAD) type II. A total 30 μg of isolated proteins from kidney cortexes was transferred to polyvinylidine difluoride (PVDF) membranes. Bands positive for PAD type II scarcely appeared in sham-operated (Sham-left) or unobstructed kidneys of unilateral ureteral obstruction (UUO) group (UUO-right). In contrast, a clear band at approximately 70 kD was observed in left kidneys 1 week after UUO (UUO-left) (*A*). Thereafter, the membrane was stained by Coomassie brilliant blue (CBB) (*B*). Although bands at approximately 60 kD and 80 kD were more intense in left kidneys of the UUO group than others, intensities of other bands were similar. When the membranes stained by rabbit serum as a first antibody instead of anti PAD type II antibody, no bands were visible (*C*). Therefore, the band in (A) is specific. That membrane was stained by CBB (*D*). When protein bands were quantified by densitometry, PAD type II amount was significantly increased in left obstructed kidneys (UUO-left) compared with that in sham-operated kidneys (Sham-left) or contra-lateral kidneys (UUO-right) (Fig 4E). $^*P < 0.01$ versus sham-operated kidneys and right contra-lateral kidneys with UUO. Values are mean ± SEM.

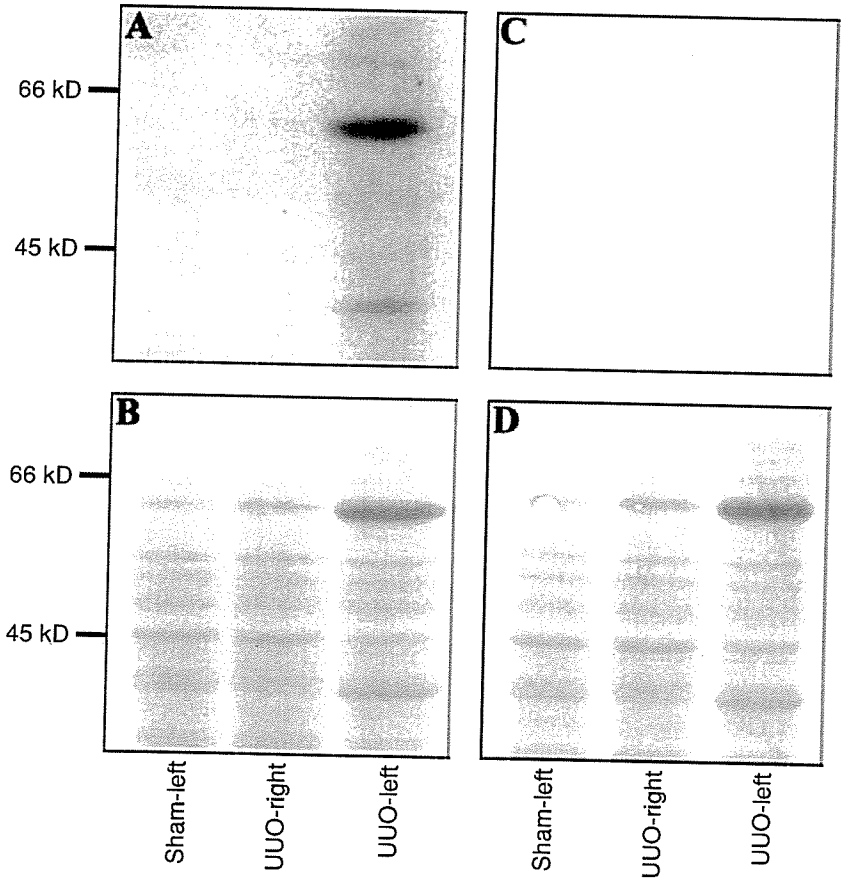

Fig. 5. Western blot for detection of citrullinated proteins. A total 30 μg of proteins isolated from kidney cortex was transferred to polyvinylidine difluroride (PVDF) membranes. For detection, monoclonal antibody was added to react chemically with modified citrulline. One membrane was treated with the modification medium before the reaction with anti-modified citrulline antibody, and then citrullinated proteins were stained as described in the Methods section (*A*), followed by Coomassie brilliant blue (CBB) staining (*B*). Citrullinated proteins were detected only in obstructed kidneys (UUO-left) (A). Another membrane was stained by same first antibody and second antibody without chemical modification as a control (*C*), followed by CBB staining (*D*). No bands of citrullinated proteins were observed in the membrane without chemical modification (C), which indicated specific reaction of first antibody to chemically modified citrulline.

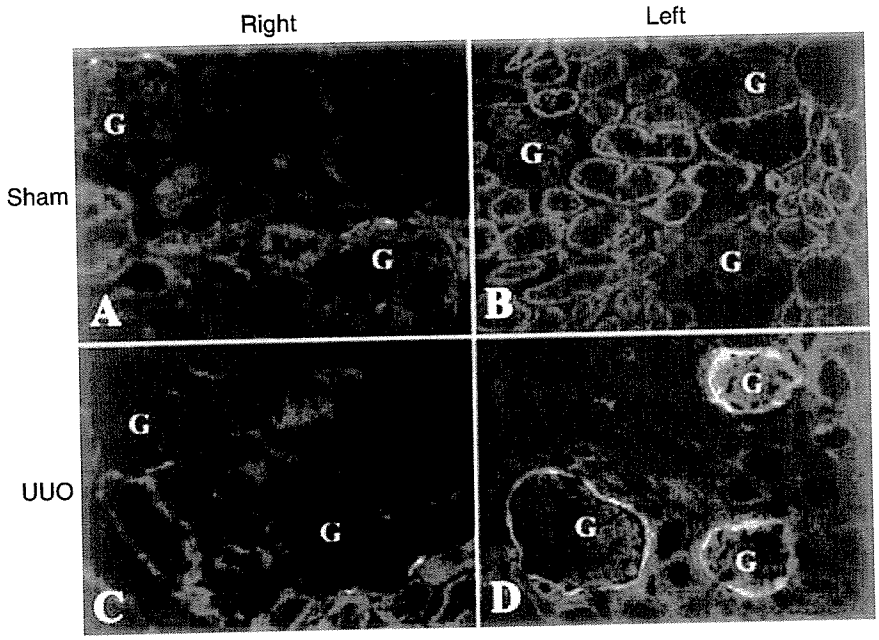

Fig. 6. Peptidylarginine deiminases (PAD) type II expression on abnormal Bowman's capsules. Kidney tissues were stained by rabbit antirat PAD type II antiserum. (*A*) Right kidney of sham-operated group. (*B*) Left kidney of sham-operated group. (*C*) Right kidney of unilateral ureteral obstruction (UUO) group. (*D*) Left kidney with ureteral obstruction of UUO group. In both sides of kidneys in sham-operated group, PAD type II expression was miniscule (A and B). In contralateral, unobstructed kidney (right), the expression was also scarce (C). On the other hand, in left kidneys staining for PAD type II was positive and located preferentially in parietal epithelial cells of Bowman's capsules (D). G is a glomerulus (original magnifications ×200).

Table 1. Summary of histologic examinations (the semiquantitative values of staining intensity and percentages of positive glomeruli for peptidylarginine deiminase (PAD) type II and citrullinated proteins

Group	PAD II		Citrullinated protein	
	Intensity	%	Intensity	%
Sham left ($N = 6$)	0.63 ± 0.14	36.9 ± 3.7	0.13 ± 0.04	9.2 ± 2.9
UUO right 1 week ($N = 6$)	0.76 ± 0.12	40.7 ± 4.5	0.08 ± 0.03	8.1 ± 2.7
UUO left 1 week ($N = 6$)	$3.64 \pm 0.13^{a,c}$	$100 \pm 0^{a,c}$	$1.71 \pm 0.06^{a,c}$	$92.1 \pm 1.8^{a,c}$
UUO left 5 week ($N = 4$)	$4.00 \pm 0.00^{a,c}$	$100 \pm 0^{a,c}$	$3.02 \pm 0.24^{a,c,d}$	$100 \pm 0^{a,c,d}$
Bypass left 5 week ($N = 4$)	$2.61 \pm 0.22^{a,c,d,e}$	$80.1 \pm 3.8^{a,b,c,d,e}$	$0.33 \pm 0.06^{b,c,d,e}$	$27.8 \pm 6.0^{b,c,d,e}$

UUO is unilateral ureteral obstruction; Bypass left 5 weeks, the data from rats receiving ureter-bladder bypass 1 week after UUO and then living for 4 weeks. The calculation methods of staining intensity and percentages were explained in the **Methods** section. Values are mean ± SEM. Statistical significance between groups was determined by the unpaired *t* test.

[a] $P < 0.01$ versus sham; [b] $P < 0.05$ versus sham; [c] $P < 0.01$ versus right contralateral kidneys of UUO group for 1 week (UUO right 1week); [d] $P < 0.01$ versus left obstructed kidneys after 1-week ligation (UUO left 1weed); [e] $P < 0.01$ versus left obstructed kidneys after 5 weeks of UUO (UUO left 5 weeks).

microscopic study showed that the lesions in Bowman's capsules with UUO were attenuated by the ureter-bladder anastomosis to release the ureteral obstruction. Five weeks after UUO operation, PAD type II expression was strongly observed in the whole parietal epithelial cells (Fig. 8C) (Table 1). This intense expression of PAD type II was significantly attenuated by the release of ureteral obstruction (Fig. 8D) (Table 1). Citrullinated proteins were also increased in Bowman's capsules of obstructed kidneys for 5 weeks (Fig. 8E) (Table 1). However, when we performed the operation for release of UUO 1 week after the ureteral ligation, the citrullinated proteins were diffusely decreased below those in kidneys with UUO for 5 weeks. Furthermore, PAD type II and citrullinated proteins were also significantly diminished in the left kidneys of the group that underwent the ureter-bladder bypass operation even compared with those in the left obstructed kidneys for 1 week, in which these proteins were already increased in Bowman's capsules (Table 1).

Actin filaments should be citrullinated in the kidney

Next, two-dimensional electrophoresis was performed to investigate what proteins were citrullinated in the kidney. We obtained two spots which were citrullinated (Fig. 9). Their molecular weights were both approximately 40 kD. The MALDI mass fingerprint spectrums of these spots at 40 kD (Fig. 10A) were analyzed by the MASCOT search engine. The results showed that citrullinated proteins at 40 kD were actins (Fig. 10B).

DISCUSSION

This report describes for the first time that PAD type II and citrullinated proteins are suitable markers for Bowman's capsules, since their expression occurs preferentially in Bowman's capsules of the renal glomeruli and increases markedly during the course of obstructive nephropathy.

For this study, we adapted a model of obstructive renal damage by unilaterally ligating the left ureter (UUO) in

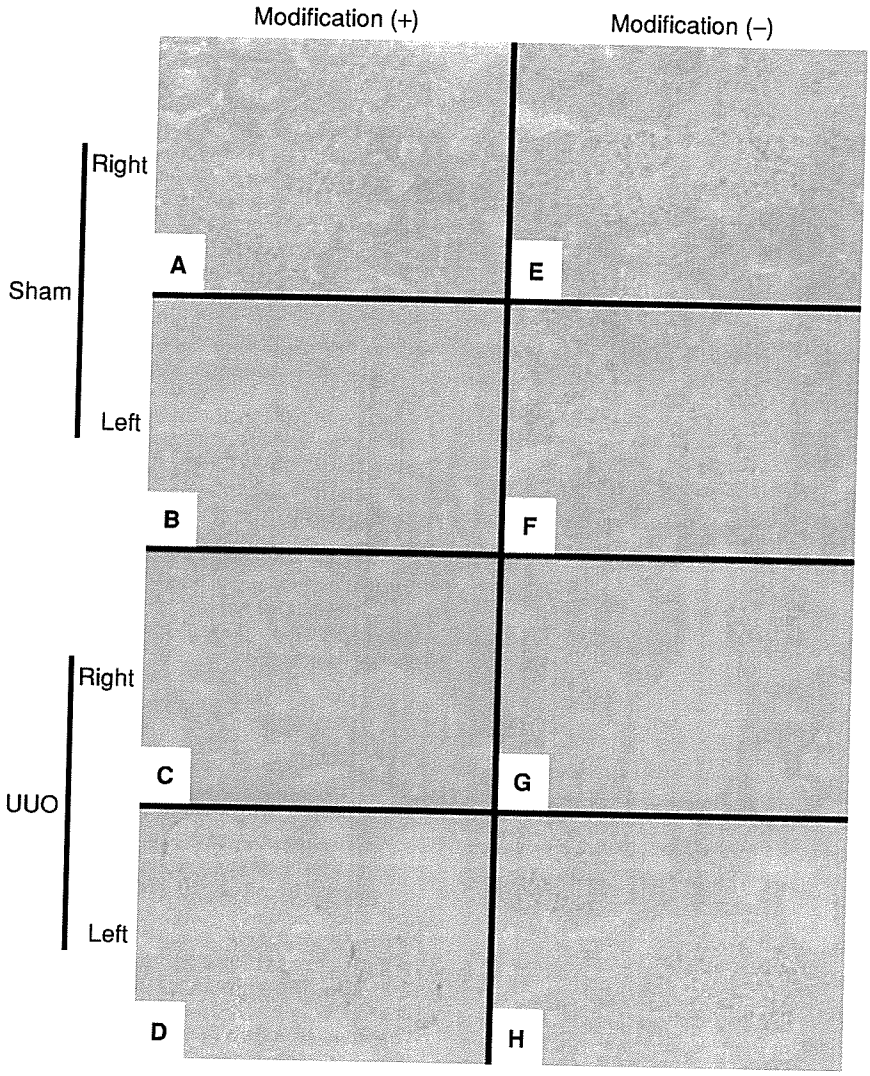

Fig. 7. Detection of citrullinated protein in situ. Citrullinated proteins were detected by modification of citrulline residues in tissues followed by staining with anti modified citrulline antibody. (*A* and *E*) Right kidney of sham-operated group. (*B* and *F*) Left kidney of sham-operated group. (*C* and *G*) Right unobstructed kidney of unilateral ureteral obstruction (UUO) group. (*D* and *H*) Left obstructed kidney of UUO group. When tissues were stained after chemical modification (A to D), both sides of sham-operated group and right kidney of UUO group did not show positive staining for citrullinated proteins (A to C). Only in the left obstructed kidney of the UUO group was protein citrullination was preferentially detected in Bowman's capsule, which appeared like rings (D). When tissues were not chemically modified (E to H), no positive staining followed (original magnifications ×200).

each of six rats and simultaneously performed sham operations as a control ($N = 6$). UUO increases fluid pressure in the urinary tract, thereby also increasing pressure in tubuli and Bowman's space. This model has been used often to study the mechanisms of renal fibrosis [16]. In the glomeruli, UUO makes parietal epithelial cells of Bowman's capsule receive tension as mechanical stress. In this study, UUO of the rat urinary tract caused renal failure within 1 week, as confirmed by increases of serum BUN and creatinine (Fig. 1). In addition, the obstructed kidneys had thickening of Bowman's capsules and cuboidal formation of the parietal epithelial cells (Fig. 2).

The results of RT-PCR to identify PADs indicated that neither PAD type I nor type III was expressed in any kidneys, whether normal, UUO operated, or sham operated (Fig. 3). Similarly, PAD type IV was rarely detected in any of these kidneys (Fig. 3), and even this limited expression of PAD type IV mRNA seemed to come from circulating leukocytes left after presurgical perfusion, because these cells do express PAD type IV [17]. A marked difference was the expression of PAD type II mRNA found in both right and left kidneys of the UUO group and the sham-operated group (Fig. 3). Therefore, we judged that renal cells express only type II of the four known PAD types. When we measured the densities of bands and calculated relative amounts of PAD type II mRNA/GAPDH mRNA, amounts in the rats' left obstructed kidneys were significantly higher than in any other samples of kidneys from sham-operated rats or right kidneys from the UUO group (Fig. 3E). This increase of PAD type II in obstructed kidneys was confirmed by Western blot of protein levels (Fig. 4). Sham-operated and unobstructed kidneys had only negligible levels of PAD type II, whereas the bands of PAD type II were readily detected at the expected molecular weight in all obstructed kidneys from the UUO group. Therefore, PAD type II is expressed by renal cells, and the amount increases after ureteral blockage (Fig. 4E). In addition, glomerular parietal epithelial cells of obstructed kidneys preferentially express PAD type II, but those of normal kidneys (Fig. 6). Because

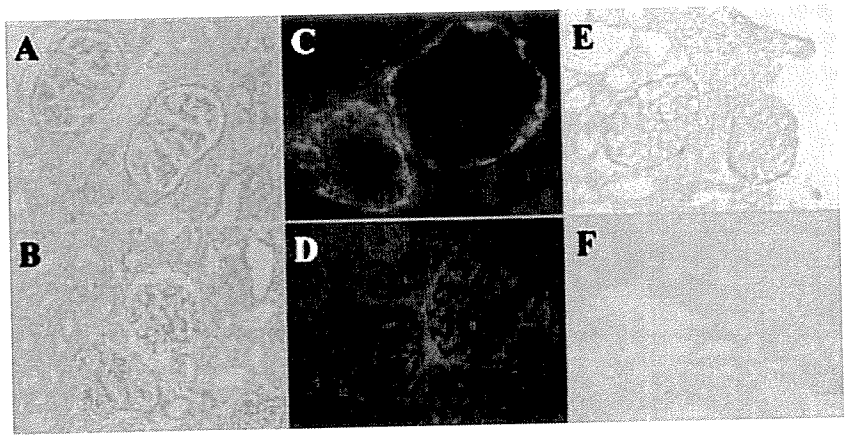

Fig. 8. Representative sections stained for periodic acid-Schiff (PAS) (*A* and *B*), peptidylarginine deiminases (PAD) type II (*C* and *D*), and citrullinated protein (*E* and *F*) of rats that lived with unilateral ureteral obstruction (UUO) for 5 weeks (A, C, and E) or that received operation to release the ureteral obstruction by ureter-bladder bypass 2 week after UUO operation and then lived for 4 weeks (B, D, and F). Under light microscope, although glomeruli of obstructed kidneys had thickened Bowman's capsules and cuboidal changes of parietal epithelium (A), these changes returned to normal in rats receiving bypass operation, in which parietal epithelial cells were simple and flat squamous (B). PAD type II expression was strongly observed preferentially in parietal epithelial cells around the whole Bowman's capsule of rats with UUO (C). On the other hand, parietal epithelial cell of rats with the ureter-bladder bypass expressed much less PAD type II (D). Similarly, citrullinated proteins were clearly detected preferentially in Bowman's capsules of rats with UUO for 5 weeks (E). By the ureter-bladder bypass, citrullinated proteins in Bowman's capsules were apparently decreased (F).

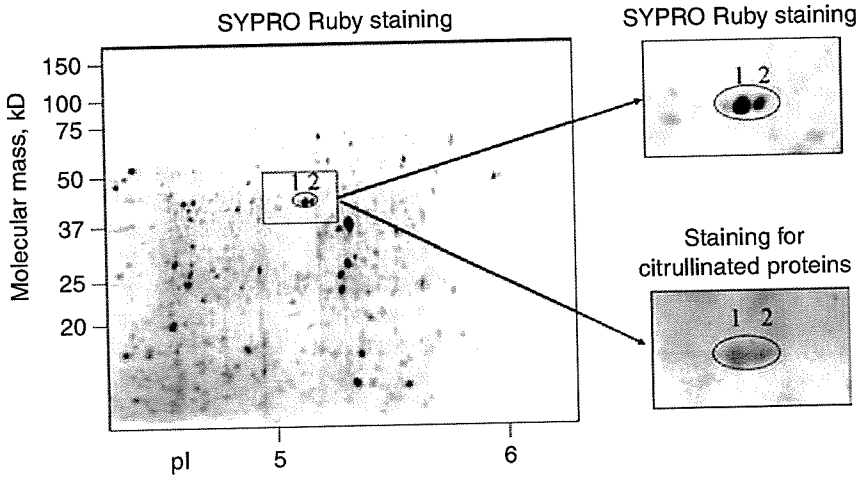

Fig. 9. Sypro ruby stained protein map of rat kidney with unilateral ureteral obstruction (UUO). A total of 100 μg protein was separated using 18 cm pH 4 to 7 immobilized pH gradients (IPG) and 7.5% sodium dodecyl sulfate-polyacrylamide gel electrophoresis (SDS-PAGE). The proteins were resolved by differential isoelectric point (pI) for the first dimensional running (x axis) and differential molecular weight (MW) for the second dimension (y axis). Proteins were stained with sypro ruby gel stain. To detect citrullinated protein, after sypro ruby staining of two-dimensional electrophoresis gel, proteins were transferred onto polyvylidine difluoride (PVDF) membrane and incubated with antibody. Two protein spots were detected (spot 1, 2). Enlarged region of sypro ruby stained two-dimensional electrophoresis gel are in right side. Sypro ruby staining is shown in the upper side and staining for citrullinated protein is shown in lower side.

the right unobstructed kidneys from UUO-treated rats scarcely expressed PAD type II, the significant increase of PAD type II only in the left obstructed kidneys (Table 1) evidently arose from the mechanical stress of ureteral obstruction, not circulating factors.

PADs catalyze the citrullination reaction, which converts protein arginine to citrulline residues in a Ca^{2+}-dependent manner [11]. Possibly related is a previous report that endothelin and platelet-activating factor (PAF) act on the parietal sheet of Bowman's capsule by increasing intracellular concentrations of Ca^{2+} [18]. In addition, endothelin and PAF were induced by ureteral obstruction [16, 19]. On the basis of those reports, presumably intracellular Ca^{2+} concentrations rise in parietal epithelial cells of Bowman's capsule after ureteral obstruction, and this elevated concentration would be available to function with PAD type II in the increased catalysis of protein citrullination at that site (Fig. 7). Therefore, when we assessed our three groups of kidneys with Western blotting, citrullinated proteins were detected only in kidneys with ureteral obstruction (Fig. 5). Although PAD type II expression was clearly detected in cytoplasms of parietal epithelial cells, we could not decide whether citrullinated proteins were located in the parietal epithelium or the basement membrane of Bowman's capsules. In future, immunoelectron microscopy will reveal the location.

Our studies using UUO model for 1 week indicated that citrullination occurs preferentially in Bowman's capsules of the renal glomeruli and increases markedly during the course of obstructive nephropathy. Next, to

A

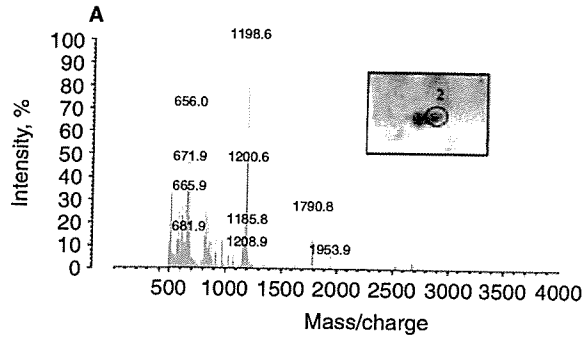

B

Protein identities and peptide masses

Protein	SWISS-PROT Accession no.	Mr (Da)	pI	Coverage	Score	Matched masses
Actin (spot 2)	P60711	42052	5.29	45%	123	976.34 2155.95 2382.83 1198.61 1354.57 800.36 1953.88 2295.08 3199.25 1639.69 1629.70 1790.77 2093.88 1580.64 1036.53 795.59 923.43

Fig. 10. Identification of protein spots by matrix-assisted laser desorption/ionization time-of flight (MALDI/TOF) mass spectrometry analysis. MALDI mass fingerprint spectrum of spot 2 was shown in the upper (*A*). Peptide mass fingerprinting was performed using the MASCOT search engine (www.matrixscience.com) based on the SWISS-PROT database. Results of the search are shown in the bottom. Protein spot 2 was identified as actin (*B*) and spot 1 was also actin [SWISS-PROT accession no. P60711 (data not shown)].

investigate whether expression of PAD type II and citrullinated proteins reflects damages of Bowman's capsules by ureteral obstruction, a ureter-bladder anastomosis to release the obstruction was made 1 week after UUO operation. Four weeks after the bypass, the appearance of Bowman's capsules returned to normal under the light microscope (Fig. 8B). On the other hand, Bowman's capsules of kidneys 5 weeks after UUO were severely thickening and had cuboidal epithelial cells (Fig. 8A). By the ureter-bladder bypass, PAD type II expression of parietal epithelial cells was significantly decreased compared with that in UUO kidneys not only for 5 weeks but also for 1 week (Fig. 8) (Table 1). Similarly, citrullinated proteins were also markedly attenuated in kidneys with the bypass compared with those in kidneys with UUO for 5 weeks and for 1 week (Fig. 8) (Table 1). These results indicate that besides being markers of Bowman's capsules, PAD type II, and citrullinated proteins can reflect the damages of Bowman's capsules. In crescentic glomerulonephritis, Bowman's capsules become similarly cuboidal. Therefore, we histologically examined rats that were induced crescentic glomerulonephritis by rabbit antiglomerular basement membrane antibody to investigate whether citrullination in Bowman's capsules participates in cuboidal formation of parietal epithelial cells. Our study showed that PAD type II and citrullinated proteins were not detected in their Bowman's capsules (data not shown). Therefore, although it was speculated that increment of citrullination in Bowman's capsules should specifically occur in response to mechanical stress to glomeruli, it remains to be solved what roles citrullination in the kidney plays.

Western blotting (Fig. 5) located several sites of citrullinated proteins in the obstructed kidneys examined here. To explain the roles of citrullination in the kidney, we performed proteome analysis of these citrullinated proteins. By two-dimensional electrophoresis, two protein spots which were citrullinated were obtained (Fig. 9). Their molecular weights were approximately 40 kD although main band was present at approximately 60 kD rather than 40 kD in Western blotting for citrullinated proteins (Fig. 5). The analysis of mass fingerprint spectra of these spots at 40 kD revealed that these were actins (Fig. 10). Although we wanted to identify the 60 kD citrullinated protein, the protein could not be detected by two-dimensional electrophoresis (Fig. 9), probably caused by technical difficulties. Therefore, we think these proteome analyses are now incomplete. In future, 60 kD citrullinated proteins should be identified to explain further fundamental roles of citrullination in kidneys. Previous reports described intermediate filaments of cytoskeletal proteins such as keratin and vimentin that were also citrullinated [20, 21]. Such citrullination abolished the positive charge of protein molecules, inevitably causing significant alteration in their structure [4, 5]. Therefore, if citrullinated proteins in Bowman's capsule are cytoskeletal proteins, that would explain defense mechanism of Bowman's capsule against mechanical stress to glomeruli.

Only one suitable marker of Bowman's capsule has been reported previously [1]. Our study described here greatly extends that report by indicating that PAD type II and citrullinated proteins are preferentially expressed in Bowman's capsules and, additionally, that their

expression increases in damaged kidneys by ureteral obstruction. These newfound markers of Bowman's capsule are expected to broaden the experimental possibilities for research on kidney diseases.

ACKNOWLEDGMENTS

We thank Phyllis Minick for critical editing of the manuscript. We also acknowledge Dr. A. Shimizu and Dr. Y. Masuda for kindly providing tissue samples of rat anti-GBM nephritis. This study was supported a grant from the Health Science Research Grants for Comprehensive Research on Aging and Health from Ministry of Health Labor and Welfare, Japan, and a grant-in-aid for Scientific Research from Ministry of Education, Science and Culture, grant 15790436 Japan to T.I.

Reprint requests to Toshiyuki Imasawa M.D., Ph.D., Department of Internal Medicine and Division of Immunopathology, Clinical Research Center, Chiba-East National Hospital, 673 Nitona, Chuoh, Chiba, 260–8712, Japan.
E-mail: timasawa@yahoo.co.jp

REFERENCES

1. SHIRATO I, ASANUMA K, TAKEDA Y, *et al*: Protein gene product 9.5 is selectively localized in parietal epithelial cells of Bowman's capsule in the rat kidney. *J Am Soc Nephrol* 11:2381–2386, 2000
2. KUBILUS J, WAITKUS RF, BADEN HP: Partial purification and specificity of an arginine-converting enzyme from bovine epidermis. *Biochim Biophys Acta* 615:246–251, 1980
3. ROGERS GE, SIMMONDS DH: Content of citrulline and other amino acids in a protein of hair follicles. *Nature* 182:186–187, 1958
4. MOSCARELLO MA, PRITZKER L, MASTRONARDI FG, WOOD DD: Peptidylarginine deiminase: A candidate factor in demyelinating disease. *J Neurochem* 81:335–343, 2002
5. STEINERT PM, PARRY DA, MAREKOV LN: Trichohyalin mechanically strengthens the hair follicle: Multiple cross-bridging roles in the inner root shealth. *J Biol Chem* 278:41409–41419, 2003
6. ISHIGAMI A, ASAGA H, OHSAWA T, *et al*: Peptidylarginine deiminase type I, type II, type III and type IV are expressed in rat epidermis. *Biomed Res* 22:63–65, 2001
7. SCHELLEKENS GA, DE JONG BA, VAN DEN HOOGEN FH, *et al*: Citrulline is an essential constituent of antigenic determinants recognized by rheumatoid arthritis-specific autoantibodies. *J Clin Invest* 101:273–281, 1998
8. SUZUKI A, YAMADA R, CHANG X, *et al*: Functional haplotypes of PADI4, encoding citrullinating enzyme peptidylarginine deiminase 4, are associated with rheumatoid arthritis. *Nat Genet* 34:395–402, 2003
9. ASAGA H, ISHIGAMI A: Protein deimination in the rat brain after kainate administration: Citrulline-containing proteins as a novel marker of neurodegeneration. *Neurosci Lett* 299:5–8, 2001
10. WATANABE K, SENSHU T: Isolation and characterization of cDNA clones encoding rat skeletal muscle peptidylarginine deiminase. *J Biol Chem* 264:15255–15260, 1989
11. TARCSA E, MAREKOV LN, ANDREOLI J, *et al*: The fate of trichohyalin. Sequential post-translational modifications by peptidyl-arginine deiminase and transglutaminases. *J Biol Chem* 272:27893–27901, 1997
12. ISHIGAMI A, KURAMOTO M, YAMADA M, *et al*: Molecular cloning of two novel types of peptidylarginine deiminase cDNAs from retinoic acid-treated culture of a newborn rat keratinocyte cell line. *FEBS Lett* 433:113–118, 1998
13. WATANABE K, AKIYAMA K, HIKICHI K, *et al*: Combined biochemical and immunochemical comparison of peptidylarginine deiminases present in various tissues. *Biochim Biophys Acta* 966:375–383, 1988
14. SENSHU T, SATO T, INOUE T, *et al*: Detection of citrulline residues in deiminated proteins on polyvinylidene difluoride membrane. *Anal Biochem* 203:94–100, 1992
15. SENSHU T, AKIYAMA K, KAN S, *et al*: Detection of deiminated proteins in rat skin: Probing with a monospecific antibody after modification of citrulline residues. *J Invest Dermatol* 105:163–169, 1995
16. KLAHR S, MORRISSEY J: Obstructive nephropathy and renal fibrosis. *Am J Physiol Renal Physiol* 283:F861–F875, 2002
17. ASAGA H, NAKASHIMA K, SENSHU T, *et al*: Immunocytochemical localization of peptidylarginine deiminase in human eosinophils and neutrophils. *J Leukoc Biol* 70:46–51, 2001
18. MARCHETTI J, MENETON P, LEBRUN F, *et al*: The parietal sheet of Bowman's capsule of rat renal glomerulus: A target of endothelin and PAF. *Am J Physiol* 268:F1053–F1061, 1995
19. REYES AA, KLAHR S: Renal function after release of ureteral obstruction: Role of endothelin and the renal artery endothelium. *Kidney Int* 42:632–638, 1992
20. SENSHU T, KAN S, OGAWA H, *et al*: Preferential deimination of keratin K1 and filaggrin during the terminal differentiation of human epidermis. *Biochem Biophys Res Commun* 225:712–719, 1996
21. ASAGA H, YAMADA M, SENSHU T: Selective deimination of vimentin in calcium ionophore-induced apoptosis of mouse peritoneal macrophages. *Biochem Biophys Res Commun* 243:641–646, 1998

トピックス

タンパク質のシトルリン化と病態

丸山直記**　石神昭人*

自然界にはおよそ 500 種類のアミノ酸が存在しているが，そのうちの遺伝子により規定されたわずか 20 種類のアミノ酸の組み合わせにより 10 万種類ものタンパク質を作り出す．加えて，タンパク質の翻訳後修飾は生体分子の機能の多様性を著しく増加させる．そのような翻訳後修飾の１つとして，最近注目されているタンパク質のシトルリン化がある．遺伝子に規定されたアミノ酸の１つであるアルギニンが，遺伝子に規定されないアミノ酸であるシトルリンにカルシウム依存性の酵素を介して変換され，さまざまな細胞機能や病態と関連している．この現象は，病態を把握する際の指標として応用が期待される．本稿では，その出現に生理学的側面と病理学的側面が存在していることを解説したい．

分子内のアルギニン中のグアニド基は，カルシウム依存性に酵素の peptidylarginine deiminase（PAD）によりウレイド基に変換され，シトルリンとなる（図１）．アルギニンは塩基性であるが，シトルリンに変換した後は中性となる．その結果，シトルリン化が生じたタンパク質には大きな構造的な変化が生ずる．シトルリン化による構造変化がもたらす影響は，① 電荷と抗原性の変化，② タンパク質分解酵素に対する感受性の変化，③ 細胞構造維持の変化などが挙げられる．生体組織内におけるシトルリン化タンパク質の同定は容易ではない．シトルリンは遺伝的に規定されてはいないが，生体内には常に存在しているので免疫学的寛容が誘導されており，シトルリンそのものに対する抗体の作製は極めて困難である．リウマチ患者血清には抗シトルリン化抗体が存在するので病態マーカーとなっているが，その自己抗体は免疫組織学的な応用には不十分である．我々はシトルリン特異的な化学修飾を行ったタンパク質を家兎に免疫し，特異的抗体をアフィニティーカラムにより精製した．組織中のシトルリン残基を化学修飾した後この抗体を用いることにより，シトルリン化タンパク質の特異的な検出が可能となった（図２）．

シトルリン化を担う酵素は PAD である．PAD はヒトでは１型，２型，３型，4/5型，６型の５種類のアイソタイプが同定されている．皮膚ではすべての型の PAD が発現しているが，他臓器では発現する PAD の型には特徴がある．しかし，２型はほとんどすべての臓器での発現が認められる[1]．

従来から関節リウマチ患者血清が扁平上皮細胞に免疫反応を示し，いわゆる抗ケラチン抗体

図１　PAD によるアルギニンからシトルリンへの転換

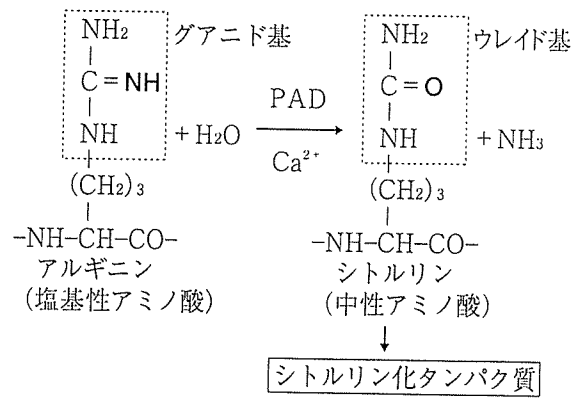

高濃度のカルシウム存在下で PAD が活性化され，アルギニン中のグアニド基がウレイド基に変換されることにより，塩基性アルギニンが中性のシトルリンとなる．PAD：peptidylarginine deiminase

* 東京都老人総合研究所　** 同 副所長

図2　表皮形成におけるシトルリン化現象と乾癬におけるシトルリン化不全

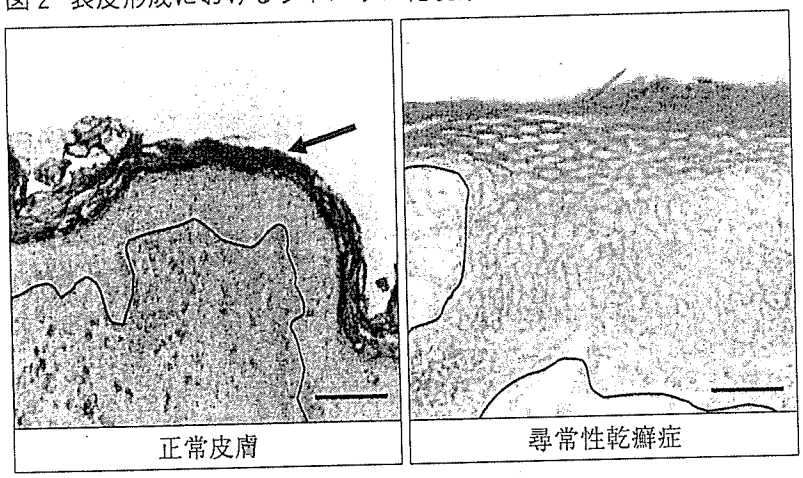

正常皮膚（左）においては表皮にシトルリン化タンパク質（→）が存在する．尋常性乾癬症（右）では，PADは発現しているがシトルリン化は極めて乏しくなっている．

として知られていた．そこで Serre の研究グループが表皮内の対応抗原を解析した結果，表皮中のフィラグリンが対応抗原であることが分かった[2]．さらに van Venrooij グループも加わり，よりシトルリン化した分子に対する自然抗体であることを報告した[3)4)]．すなわち，アルギニン残基の変換により新しい抗原決定基となったシトルリン残基に対するものであった．加えて，これまで診断に用いられていた幾つかの自己抗体がシトルリン化タンパク質に対応することも報告された．例えば抗 Sa 抗体はシトルリン化ビメンチンに特異的に反応するものであった．このように従来リウマチ患者血清に認められていた自己抗体の特性は，別の観点から整理されると思われる[5]．この事実は関節リウマチの診断に応用され，シトルリンを含み環状に配列した環状シトルリン化ペプチド（CCP）を抗原として自己抗体を検出すると，抗シトルリン化抗体が出現した場合の診断率は従来のリウマトイド因子が 61% であったのに比較して 87% となり，確定診断に利用できることが分かった．その後，1塩基多型（SNP）解析により関節リウマチと相関する遺伝子が 4/5 型 PAD であることが明らかとなり，病因解析に重要な示唆を与えた[6]．特に，4/5 型 PAD の有する基質特異性と病変の関連が注目されている[7]．病変と関連するシトルリン化タンパク質としてフィブリンが候補となっているが，今後の解析が期待される[8]．

シトルリン化現象が生体内で発見された当初は，シトルリン化による分子構造の変化は生理学的なものと考えられていた．代表的な事例としては，表皮の角化過程においてケラチンを束ねるフィラグリンがシトルリン化タンパク質となり，分解されて正常な表皮が形成されることが知られている（図2）．これは関節リウマチにおける抗シトルリン抗体の検出のきっかけとなった現象でもある．PAD の活性化にはカルシウムイオンが必須であるが，皮膚においては基底層から表皮に向かってカルシウム濃度が上昇することが知られている．このカルシウム濃度変化に伴い PAD が活性化されてシトルリン化が生じ，正常な表皮の角化が進行すると考えられている．マウス新生児表皮のシトルリン化を観察すると，胎児期から出産直後を経た約 72 時間の間にシトルリン化の消長が認められた．このことは，羊水に接している胎内から空気に満ちた外界に移る際に，シトルリン化が生理学的に重要な機能を有していることを示唆している．しかし皮膚疾患である尋常性乾癬では，このシトルリン化は著しく抑制されている（図2）．すなわち，保水性が高いアミノ酸を多く含んだフィラグリンのシトルリン化が強く抑制されているために分解されないことが病態の背景にあると推測されている[9]．この事実は，シトルリン化を生理学的な現象と見なすものであ

る．皮膚以外では神経軸索の絶縁作用をもたらすミエリン鞘の形成に，シトルリン化が重要な役割を果たしているようである[10]．すなわち，ミエリン鞘の形成時にミエリン塩基性タンパク質（MBP）が特異的にシトルリン化を受け，タンパク質の高次構造変化をもたらす．これによりオリゴデンドロサイトやシュワン細胞でミエリン鞘の形成が行われる．この事実から，シトルリン化の異常は脱髄疾患の重要な要素とも考えられている．以上に述べたように，タンパク質のシトルリン化は神経系においても生理的な機能を持つことが明らかである．

中枢神経系にはシトルリン化酵素，主に2型PADが多く発現されている．この事実から，我々は中枢神経系における病態との関連を解析した．ラットにカイニン酸を投与すると神経細胞の脱落が顕著となる．その脱落部位に対応してPAD2とシトルリン化タンパク質が出現してくる[11]．この事実は，他の神経変性疾患においても同様の現象が存在することを示唆している．そのような代表的な神経変性疾患としてアルツハイマー病がある．筆者らは臨床的にも，また神経病理学的にも明確に診断された多数のアルツハイマー病患者脳を有するブレインバンクを利用する機会を得た．これらの試料より，代表的なアルツハイマー病脳10例と年齢等が一致する9例の非アルツハイマー病脳中のシトルリン化タンパク質とPAD2の発現を比較検討した．その結果，重症のアルツハイマー病患者脳には多くのシトルリン化タンパク質が蓄積していることが明らかとなった[1]．ウエスタンブロッティングの結果は，多種類の分子種がシトルリン化していることを示していた．また，海馬領域ではPAD2発現も亢進していた．他方，対照となる非アルツハイマー病患者脳でのシトルリン化タンパク質の蓄積は極めて軽度であった．海馬領域におけるシトルリン化タンパク質の局在を検討すると，分子細胞層と歯状回の間の接合部位とCA1およびCA2領域に認められた．またPAD2もほぼ同一部位において発現が亢進していた．シトルリン化タンパク質およびPAD2の染色性からアストロサイトにも局在していることが示唆されたので，GFAPとの二重染色を行ったところ完全に一致した．表皮の角化におけるフィラグリンに対応する脳内のタンパク質を同定するためにMALDI-TOF-MS解析を行った．その結果，多数のシトルリン化タンパク質の一部として，中間径フィラメントのビメンチンとGFAPが同定された．すでにシトルリン化されたビメンチンは中間径フィラメントの機能を失うという報告もあり，細胞機能に重要な影響をもたらすことが示唆された[12]．

PADはほぼ全身に分布し，また神経変性疾患においてシトルリン化タンパク質が重要な指標となることから，他の臓器障害においても同様の現象が出現している可能性がある．最近我々は，ラットの片側尿管を1週間結紮すると，結紮された側の腎臓にシトルリン化タンパク質の出現とPAD2の発現亢進を認めた．その局在を検討すると，PAD2は糸球体ボーマン嚢上皮細胞に特異的に発現亢進が認められた．また，シトルリン化タンパク質はボーマン嚢周囲の間質に検出された．しかし結紮開放後，時間が経つと次第に両者が観察されなくなったことから，病勢を反映していると思われる[6]．この解析ではシトルリン化とPAD2の発現は糸球体ボーマン嚢に限局しており，その組織特異性も極めて強く，興味深い結果である．ヒトの腎疾患でもシトルリン化タンパク質を検出することから，神経変性疾患ばかりではなく，シトルリン化が広範囲の臓器において病理的な指標となることを示唆している．

文　献

1) Ishigami A, et al: Abnormal accumulation of citrullinated proteins catalyzed by peptidylarginine deiminase in hippocampal extracts from patients with Alzheimer's disease. J Neurosci Res 80: 120–128, 2005.

2) Simon M, et al: The cytokeratin filament-aggregating protein filaggrin is the target of the so-called "antikeratin antibodies," autoantibodies specific for rheumatoid arthritis. J Clin Invest 92: 1387-1393, 1993.
3) Schellekens G A, et al: Citrulline is an essential constituent of antigenic determinants recognized by rheumatoid arthritis-specific autoantibodies. J Clin Invest 101: 273-281, 1998.
4) Girbal-Neuhauser E, et al: The epitopes targeted by the rheumatoid arthritis-associated antifilaggrin autoantibodies are posttranslationally generated on various sites of (pro)filaggrin by deimination of arginine residues. J Immunol 162: 585-594, 1999.
5) Vossenaar E R, et al: Rheumatoid arthritis specific anti-Sa antibodies target citrullinated vimentin. Arthritis Res Ther 6: R142-R150, 2004.
6) Suzuki A, et al: Functional haplotypes of PADI4, encoding citrullinating enzyme peptidylarginine deiminase 4, are associated with rheumatoid arthritis. Nat Genet 34: 395-402, 2003.
7) Nakayama-Hamada M, et al: Comparison of enzymatic properties between hPADI2 and hPADI4. Biochem Biophys Res Commun 327: 192-200, 2005.
8) Masson-Bessiere C, et al: The major synovial targets of the rheumatoid arthritis-specific antifilaggrin autoantibodies are deiminated forms of the alpha- and beta-chains of fibrin. J Immunol 166: 4177-4184, 2001.
9) Ishida-Yamamoto A, et al: Sequential reorganization of cornified cell keratin filaments involving filaggrin-mediated compaction and keratin 1 deimination. J Invest Dermatol 118: 282-287, 2002.
10) Gould R M, et al: Messenger RNAs located in myelin sheath assembly sites. J Neurochem 75: 1834-1844, 2000.
11) Asaga H, et al: Protein deimination in the rat brain after kainate administration: citrullin-containing in cerebrum as a novel marker of neurodegeneration. Neurosci Lett 299: 5-8, 2001.
12) Inagaki M, et al: Ca^{2+}-dependent deimination-induced disassembly of intermediate filaments involves specific modification of the amino-terminal head domain. J Biol Chem 264: 18119-18127, 1989.
13) Feng D, et al: Citrullination preferentially proceeds in glomerular Bowman's capsule and increases in obstructive nephropathy. Kidney Int 68: 84-95, 2005.

Citrullinated Proteins in Diseases

Naoki Maruyama, Akihito Ishigami
Tokyo Metropolitan Institute of Gerontology